Touching the High Complexity of Prebiotic Vivinal Galacto-oligosaccharides Using Porous Graphitic Carbon Ultra-High-Performance Liquid Chromatography Coupled to Mass Spectrometry

Logtenberg, Madelon J; Donners, Kristel M H; Vink, Jolien C M; van Leeuwen, Sander S; de Waard, Pieter; de Vos, Paul; Schols, Henk A

Published in:
Journal of Agricultural and Food Chemistry

DOI:
10.1021/acs.jafc.0c02684

Publication date:
2020

JOURNAL OF AGRICULTURAL AND FOOD CHEMISTRY

pubs.acs.org/JAFC

Article

Touching the High Complexity of Prebiotic Vivinal Galacto-oligosaccharides Using Porous Graphitic Carbon Ultra-High-Performance Liquid Chromatography Coupled to Mass Spectrometry

Madelon J. Logtenberg, Kristel M. H. Donners, Jolien C. M. Vink, Sander S. van Leeuwen, Pieter de Waard, Paul de Vos, and Henk A. Schols*

Cite This: *J. Agric. Food Chem.* 2020, 68, 7800−7808

Read Online

ACCESS | Metrics & More | Article Recommendations | Supporting Information

ABSTRACT: Galacto-oligosaccharides (GOS) are used in infant formula to replace the health effects of human milk oligosaccharides, which appear to be dependent upon the structure of the individual oligosaccharides present. However, a comprehensive overview of the structure-specific effects is still limited as a result of the high structural complexity of GOS. In this study, porous graphitic carbon (PGC) was used as the stationary phase during ultra-high-performance liquid chromatography−mass spectrometry (UHPLC−MS). This approach resulted in the recognition of more than 100 different GOS structures in one single run, including reducing and non-reducing GOS isomers. Using nuclear magnetic resonance-validated structures of GOS trisaccharides, we discovered MS fragmentation rules to distinguish reducing isomers with a mono- and disubstituted terminal glucose by UHPLC−PGC−MS. UHPLC−PGC−MS enabled effective recognition of structural features of individual GOS components in complex GOS preparations and during, e.g., biological conversion reactions. Hence, this study lays the groundwork for future research into structure-specific health effects of GOS.

KEYWORDS: *galacto-oligosaccharides, preparative chromatography, tandem mass spectrometry, porous graphitic carbon, liquid chromatography*

1. INTRODUCTION

Postnatal nutrition has a lifelong impact on health and well-being because it guides the development of complex interactions between the intestinal microbiota and the gastrointestinal immune system.[1,2] Although breast milk is still considered the gold standard, many types of infant formula are nowadays commercially available for those infants for which exclusive breastfeeding is not an option. Oligosaccharides present in human milk (HMOs) function as prebiotics and have a direct effect on immunity by supporting the development of the gut barrier.[3,4] Currently, only a limited number of less complex HMOs, such as 2′-fucosyllactose (2′FL), 3′-sialyllactose (3′SL), and lacto-*N*-tetraose (LNT), are commercially available and applied in infant formula.[5] Therefore, predominantly galacto-oligosaccharides (GOS) and the less complex fructo-oligosaccharides (FOS) are used as substitute to replace the health effects of HMOs in infant formula.[6]

GOS are produced by hydrolysis and transgalactosylation of lactose, in which the process is catalyzed by β-galactosidase.[7] This results in galactose chains with a terminal reducing glucose or galactose unit, varying in the degree of polymerization (DP) from 2 to 8 and in the type of glycosidic linkage: $\beta(1-2)$, $\beta(1-3)$, $\beta(1-4)$, and $\beta(1-6)$.[7] Besides GOS with a free anomeric carbon at the terminal position (reducing GOS), also non-reducing GOS containing the structural motif α-D-Glc*p*-(1↔1)-β-D-Gal*p* or β-D-Glc*p*-(1↔1)-β-D-Gal*p* have been reported.[8−10] The source of the enzyme has a large influence on both the regioselectivity of the enzyme and the size of the produced oligosaccharides, resulting in mixtures enriched in either $\beta(1-3)$-, $\beta(1-4)$-, or $\beta(1-6)$-linked galactose residues.[11] Because the applied enzymes vary in industry, several structurally distinct GOS mixtures are commercially available.[12,13]

The prebiotic effects of GOS vary depending upon its monomer composition, type of glycosidic linkage, and DP.[14−15,17−18] For example, previous *in vitro* studies with pig and human fecal microbiota showed the preference of microbiota for degradation of $\beta(1-2)$ and $\beta(1-3)$ linkages over $\beta(1-4)$ and $\beta(1-6)$ linkages.[14,15] In studies aiming on restoring *Bifidobacterium* levels in antibiotic-disrupted microbiota from adults, GOS DP $\geq$ 4 was more efficient than GOS DP $\leq$ 3.[14] Also, immune effects are demonstrated to depend upon the structure of GOS, because DP2 and DP3 were shown to have a higher protective effect on the intestinal barrier integrity than higher DPs.[16] However, to date, there is little

Received: April 28, 2020
Revised: June 10, 2020
Accepted: June 17, 2020
Published: June 17, 2020

evidence of the exact relationship between the structure of individual GOS components and their prebiotic and immune effects,[14−18] which could be partly explained by the lack of high-throughput characterization methods, which enable the recognition of individual GOS components in complex GOS preparations and during, e.g., biological conversion reactions.

Over the past decade, several studies described the characterization of GOS using techniques, such as hydrophilic interaction chromatography (HILIC) coupled to mass spectrometry (MS)[13] and preparative HILIC of DP fractions prior to ^{1}H and ^{13}C nuclear magnetic resonance (NMR) analysis.[9] The study by van Leeuwen et al.[8] offers probably the most comprehensive overview thus far of the different components present in Vivinal GOS, a commercial GOS mixture produced by a *Bacillus circulans* β-galactosidase.[19] Preparative high-performance anion-exchange chromatography combined with pulsed amperometric detection (HPAEC−PAD) of DP fractions prior to ^{1}H and ^{13}C NMR analysis revealed more than 40 different components.[8] The employed *B. circulans* β-galactosidase introduced β(1−2), β(1−3), β(1−4), and β(1−6) elongations on the reducing glucose residue. However, longer oligosaccharides (DP ≥ 4) were reported to be mainly β(1−4) elongations of acceptor di- and trisaccharides by β-D-Gal*p*.[8,11]

Nonetheless, HPAEC-based characterization methods alone might not be suitable for structure−function studies, in which the complex relation between the structure of GOS and a specific bioactivity is monitored. Co-elution of isomers and GOS structures having a different DP hinders the annotation of individual GOS.[8] Labor-intensive size-exclusion chromatographic (SEC) fractionation of GOS into its constituent DPs prior to analysis will help but is not suitable for structure−function studies. Porous graphitic carbon (PGC) chromatography could potentially overcome this limitation. The retention mechanism of this stationary phase is based on the size, type of linkage, and resulting three-dimensional (3D) structure of oligosaccharides.[20] As such, PGC chromatography provides adequate separation of GOS and HMOs and has a high sensitivity.[21,22] The excellent chromatographic resolution even resulted in the partial separation of α- and β-anomers,[23] although complicating the already complex elution pattern. Reduction of the oligosaccharides prior to analysis avoids the occurrence of such double peaks, while maintaining a good separation of the different oligosaccharides.[22]

PGC with ultra-high-performance liquid chromatography (UHPLC) is highly compatible with MS, which enables the characterization of galacto-oligosaccharides based on *m*/*z* and MS^2 fragmentation spectra. Nonetheless, MS fragmentation pathways of derivatized galacto-oligosaccharides are highly complex and partly unknown.[13,24] Hence, NMR generally proves to be highly valuable for the conclusive characterization of oligosaccharides.[25]

In this study, a high-throughput characterization method was developed for GOS based on UHPLC−PGC−MS. Both SEC and preparative UHPLC−PGC−MS were applied to obtain pure isomers representing different isomer classes. These isomers were analyzed with NMR to be able to connect the structure to the observed MS^2 fragmentation. The developed characterization method will provide novel insight in the complexity of GOS mixtures currently applied in infant formula and ultimately will contribute to a better understanding of structure-specific health effects of GOS.

2. MATERIALS AND METHODS

2.1. Materials. Purified Vivinal GOS was kindly provided by Friesland Campina DOMO (Beilen, Netherlands). Vivinal GOS was fractionated to obtain purified Vivinal GOS with <3% (w/w, dry matter) monomers and lactose. In short, the lactose present in Vivinal GOS was hydrolyzed by lactase, followed by removal of the monosaccharides by nanofiltration.

GOS DP3 standards β-3′-galactosyl-lactose, β-4′-galactosyl-lactose, and β-6′-galactosyl-lactose were purchased from Carbosynth (Berkshire, U.K.).

2.2. Fractionation of Vivinal GOS. *2.2.1. Fractionation on DP Using Size-Exclusion Chromatography.* Vivinal GOS was fractionated on DP by size-exclusion chromatography (SEC) using an AKTA purifier system (GE Healthcare, Chicago, IL, U.S.A.). GOS (20 mg/mL, 5 mL) was injected into three serially connected Hiload 26/60 Superdex 30 preparative grade columns, each with a column volume of 300 mL (GE Healthcare). The temperature was set at 35 °C, and the flow rate was set at 2.6 mL of H_2O/min. A refractive index (RI) detector (Shodex RI-72, Yokohama, Japan) was used to monitor the elution. The eluent containing GOS was collected in 5 mL fractions using a Frac-950 fraction collector (GE Healthcare). Subsequently, fractions were analyzed using matrix-assisted laser desorption/ionization time-of-flight mass spectrometry (MALDI−TOF−MS) as described previously[26] to determine the molecular weight of GOS present in the fractions. The fractions with a purity of at least 90% according to the signal intensity as measured by MALDI−TOF−MS were pooled. Fractions containing DP3, which eluted between 720 and 740 mL, of multiple runs were pooled and freeze-dried. On the basis of the elution pattern and *m*/*z*, also DP1, DP2, DP4, DP5, DP6, and DP ≥7 were combined per DP and freeze-dried. Weights obtained per DP were used to determine the relative abundance of the different DPs in purified Vivinal GOS.

2.2.2. Reduction of Purified GOS DP3. Prior to further fractionation, 100 mg of purified GOS DP3 was subjected to reduction conditions and subsequently purified by solid-phase extraction (SPE). Freshly prepared 0.5 M sodium borohydride ($NaBH_4$) was added to GOS DP3 (1.25 mg/mL) in a ratio of 1:1 (v/v) and incubated overnight at room temperature. Cartridges (bed weight, 250 mg; column volume, 3 mL; Carbograph, Supelclean ENVI carb; Sigma-Aldrich, St. Louis, MO, U.S.A.) were activated with 1.5 mL of 80:20 (v/v) acetonitrile (ACN)/H_2O, followed by 4× 1.5 mL of H_2O. The reduced GOS DP3 including non-reducing isomers [(1−1) linkage] (10 mL) were loaded on the cartridge, after which the cartridge was washed 2 times with 2 mL of H_2O. Subsequently reduced (including non-reducing) GOS DP3 were eluted with 2× 1.5 mL of 40:60 (v/v) ACN/H_2O. Eluted reduced (including non-reducing) GOS were dried at 30 °C under nitrogen gas, resolubilized in H_2O, and freeze-dried.

2.2.3. Fractionation of Reduced (Including Non-reducing) DP3 Using Preparative UHPLC−PGC−MS. Fractionation was performed on a Waters preparative LC−MS system, equipped with a 2767 sample manager, 2545 quaternary gradient module, fluid organizer, 3100 mass detector, and 2998 photodiode array detector (Waters, Milford, MA, U.S.A.). Reduced (including non-reducing) GOS DP3 (95 mg/mL, 0.5 mL) was centrifuged (5 min, 15000*g*) and injected onto a PGC column (150 × 21.2 mm, 5 μm particle size, Hypercarb; Thermo Scientific, San Jose, CA, U.S.A.). The flow rate was set at 18.34 mL/min. Mobile phase A consisted of ULC−MS water + 0.1% (v/v) formic acid, and mobile phase B consisted of ACN + 0.1% (v/v) formic acid. The gradient applied was as follows: 0−80.8 min, 3−11% B; 80.8−95.3 min, 11−100% B; and 95.3−109.9 min, 100−3% B, followed by equilibration at 3% B. Fractions of 6.1 mL were collected and analyzed using analytical UHPLC−PGC−MS (see section 2.3.2). Fractions were pooled on the basis of the retention time and MS^2 fragmentation of the isomer present. Only fractions with a purity of 90% according to the signal intensity as measured by analytical UHPLC−PGC−MS were pooled. Afterward, ACN was evaporated under a stream of nitrogen gas and the remaining water phase was freeze-dried.

https://dx.doi.org/10.1021/acs.jafc.0c02684
J. Agric. Food Chem. 2020, 68, 7800−7808

2.3. Characterization of Vivinal GOS DP3. *2.3.1. Determination of Monosaccharide Composition of Vivinal GOS DP3.* The monosaccharide composition of reduced (including non-reducing) Vivinal GOS DP3 was determined using HPAEC−PAD. Prior to analysis, reduced (including non-reducing) Vivinal GOS DP3 was completely hydrolyzed using trifluoroacetic acid (TFA) and subsequently dissolved in 2 M TFA (0.2 mg/mL). After an incubation of 1 h at 121 °C, TFA was evaporated under a stream of air at 40 °C. The dried sample was resolubilized in water (0.025 mg/mL) and centrifuged (5 min, 15000*g*). A total of 10 μL of sample was injected to an ICS5000 system (Dionex, Sunnyvale, CA, U.S.A.) with a CarboPac PA-1 column (250 × 2 mm inner diameter), a CarboPac PA guard column (25 × 2 mm inner diameter), and a ISC5000 ED detector (Dionex) in the PAD mode. The flow rate was set at 0.4 mL/min. Mobile phases A (0.1 M sodium hydroxide), B (1 M sodium acetate in 0.1 M sodium hydroxide), and C (H_2O) were used with the following elution profile: 0−35 min, 100% C; 35.1−50 min, 100% A−40% B; 50.1−55 min, 100% B; 55.1−63 min, 100% A; and 63.1−78 min, 100% C. Post-column addition of 0.5 M NaOH at 0.1 mL/min was performed between 0 and 35 min and between 63.1 and 78 min. Galactose and glucose standards were included in the analysis. The data were analyzed using Chromeleon 7.0 (Thermo Scientific).

2.3.2. Analytical UHPLC−PGC−MS. Reduced (including non-reducing) GOS DP3 isomers were analyzed on an Accela UHPLC system (Thermo Scientific) coupled to a mass spectrometer (LTQ Velos Pro ion trap MS, Thermo Scientific) as described elsewhere, with some minor modifications.[27] Samples (0.5 μL, 0.25 mg/mL) were injected on a Hypercarb PGC column (3 μm particle size, 2.1 × 150 mm) in combination with a Hypercarb guard column (3 μm particle size, 2 × 10 mm, Thermo Scientific). As mobile phase A, ULC−MS water + 0.1% (v/v) formic acid was used. Mobile phase B consisted of ACN + 0.1% (v/v) formic acid. The flow rate was 300 μL/min. The solvents were eluted according to the following profile: 0−2 min, 3% B; 2−51.7 min, 3−11% B; 51.7−53.2 min, 11−100% B; 53.2−61 min, 100% B; 61−62.5 min, 100−3% B; and 62.5−70.3 min, 3% B. The temperatures of the autosampler and column oven were controlled at 10 and 25 °C, respectively. ULC−MS water containing 3% ACN was used to wash the autosampler needle. DP3 standards β-3-galactosyl-lactose, β-4-galactosyl-lactose, and β-6-galactosyl-lactose were used for the identification of GOS isomers. Vivinal GOS was analyzed to identify the DP3 isomers in the Vivinal GOS mixture. Prior to analysis, both the standards and Vivinal GOS were reduced and purified using a small-scale SPE method as described elsewhere.[27] Data acquisition and processing were performed using Xcalibur (version 2.2, Thermo Scientific).

2.3.3. NMR. GOS DP3 isomer fractions (approximately 100 μg) were dissolved in 1 mL of 99.8% deuterium oxide (D_2O) to exchange all protons of the sugar hydroxyl groups with deuterium. The samples were freeze-dried, dissolved in 0.7 mL of 99.8% D_2O, and transferred to a NMR tube. A small droplet of acetone was added on the top of the inside of the tube as an internal standard. This droplet was evaporated for 10 s and then mixed with the sample and set on δ = 2.225 ppm for ^{1}H spectra and δ = 31.55 ppm for ^{13}C spectra.

3. RESULTS

3.1. Vivinal GOS Is Highly Complex. The complete Vivinal GOS preparation was analyzed using UHPLC−PGC−MS after reduction of all reducing ends. Figure 1 shows the presence of a large number of oligosaccharides in Vivinal GOS. The structural complexity of Vivinal GOS becomes even more apparent when the *m*/*z* values are selected for each DP (Figure 1), which shows the large variety of isomers per DP.

The non-reducing isomers containing a (1−1) linkage were easily distinguished on the basis of a *m*/*z* difference of 2 because they could not be reduced by $NaBH_4$. Non-reducing DP3 isomers showed an overlap in retention time with reducing DP3 isomers (Figure 2). When their relatively low abundance is taken into account, most non-reducing DP3 isomers would not have been detected without reduction prior to analysis. In total, UHPLC−PGC−MS of reduced Vivinal GOS enabled the identification of 15 non-reducing and 23 reducing DP3 isomers.

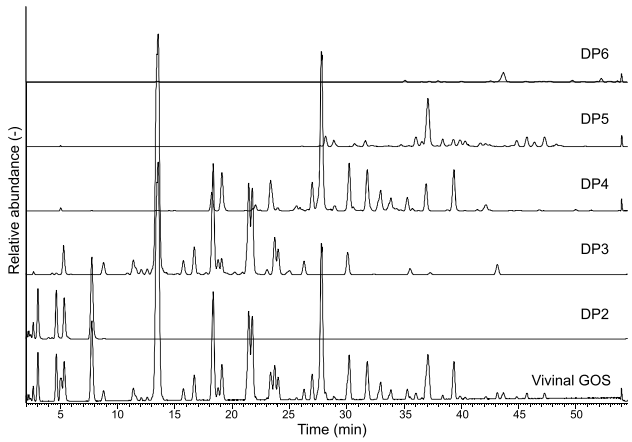

Figure 1. UHPLC−PGC−MS profile of reducing and non-reducing Vivinal GOS and DP2−6 after selection of the appropriate *m*/*z* for that DP. All elution profiles were normalized to the actual contribution of each DP to the total mixture.

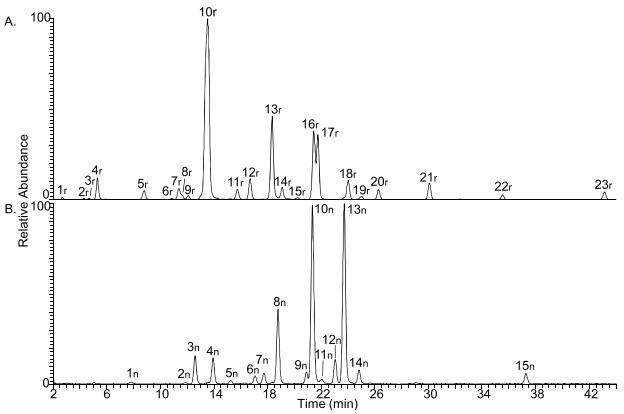

Figure 2. UHPLC−PGC−MS profile of Vivinal GOS DP3 with the selection of (A) reducing [*m*/*z* 505 and 551 (M + FA)] and (B) non-reducing [*m*/*z* 503 and 549 (M + FA)] isomers. The most abundant peak in both chromatograms was set at 100%. Peak numbers correspond to characterized GOS isomers in Table 1, with r being reducing isomers and n being non-reducing isomers [(1−1) linked].

Theoretically, each DP3 isomer could be further elongated during GOS production by β-galactosidase via either a β(1−3), β(1−4), β(1−6), or β(1−2) linkage, resulting in four distinct DP4 isomers for each distinct DP3 isomer, in which the number would be even higher when branching of the backbone is taken into consideration. However, Vivinal GOS DP4 is "only" composed of 21 reducing and 13 non-reducing isomers (Figure 3), and Vivinal GOS DP5 is "only" composed of 24 reducing and 11 non-reducing isomers (Figure 4). This finding confirms the presence of a homologue series, as reported in a previous study,[8] with longer oligosaccharides (DP ≥ 4) presented by β(1−4) elongations of acceptor di- and trisaccharides by β-D-Gal*p*. Additionally, reducing isomers are most dominant in each DP because they contributed to 86, 87, and 84% of the peak areas of DP3, DP4, and DP5, respectively.

https://dx.doi.org/10.1021/acs.jafc.0c02684
J. Agric. Food Chem. 2020, 68, 7800−7808

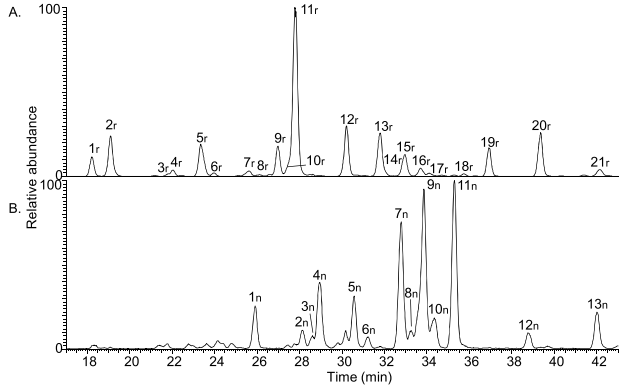

Figure 3. UHPLC−PGC−MS profile of Vivinal GOS DP4 with selection of (A) reducing [*m*/*z* 667 and 713 (M + FA)] and (B) non-reducing [*m*/*z* 665 and 711 (M + FA)] isomers. The most abundant peak in both chromatograms was set at 100%. Peak numbers of the reducing isomers (r) correspond to the different reducing GOS DP4 isomers in Table S3 of the Supporting Information. Peak numbers of the non-reducing isomers (n) only present the different non-reducing GOS DP4 isomers.

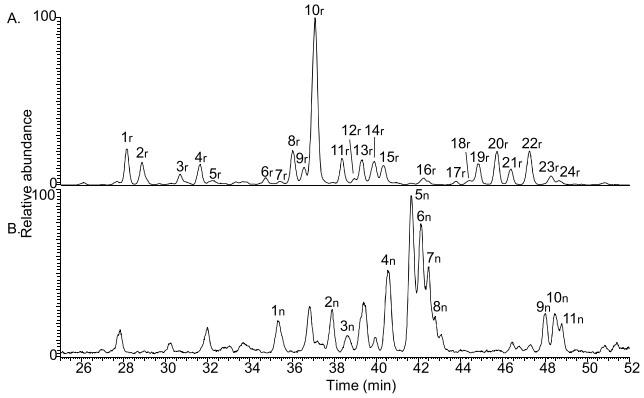

Figure 4. UHPLC−PGC−MS profile of Vivinal GOS DP5 with selection of (A) reducing [*m*/*z* 829 and 875 (M + FA)] and (B) non-reducing [*m*/*z* 827 and 873 (M + FA)] isomers. The most abundant peak in both chromatograms was set at 100%. Peak numbers present the different reducing (r) and non-reducing (n) GOS DP5 isomers.

For further characterization, the focus will be on DP3 because it will also give us insights into the structures of higher DPs.

3.2. Characterization of Vivinal GOS DP3. Characterization of GOS DP3 isomers was based on analytical UHPLC−PGC−MS covering all isomers. NMR analysis of pure isomers representing different isomer classes was performed to link the structures to the observed MS^2 fragmentation. This provides deeper insight into the fragmentation behavior of GOS. Additionally, the constituent monomer composition was determined using hydrolysis prior to HPAEC analysis. In the following paragraphs, the characterization of various isomers will be further described.

3.2.1. Characterization of Purified GOS DP3 Isomers Using NMR. NMR is used for the characterization of GOS DP3 isomers representing different isomer classes. The purity of the isomers is of importance for NMR analysis. As a result of the substantial overlap of isomers with different DP (Figure 1), Vivinal GOS was first fractionated on size (DP) using SEC to facilitate further fractionation on the isomer level. According to the weight obtained per DP, their relative abundance in Vivinal GOS was as follows: DP1, 2%; DP2, 11%; DP3, 46%; DP4, 25%; DP5, 10%; DP6, 4%; and DP > 7, 2%. The obtained GOS DP3 pool was reduced and further fractionated by preparative UHPLC−PGC−MS to obtain pure isomers. Preparative UHPLC−PGC−MS showed a similar peak resolution when compared to the analytical method (data not shown). In total, four different GOS DP3 isomers representing different isomer classes (4_r, 13_r, 21_r, and 13_n in Figure 2) were obtained for further NMR analysis in sufficient amount and purity.

From the NMR data, all ^1H and ^{13}C chemical shifts could be determined for the four isolated structures (Table S1 of the Supporting Information). The chemical shift patterns of the two Gal residues B and C of structures 4_r and 13_r fit with data expected for non-reducing terminal β-D-Gal*p* residues. This suggests a structure with two terminal Gal residues, indicating a disubstituted glucitol residue A.[8] For structure 4_r, the glucitol residue A showed H-2;C-2 and H-4;C-4 chemical shifts that significantly shifted from the literature data for glucitol,[28] indicating a disubstituted glucitol residue at positions O-2 and O-4. The heteronuclear multiple-bond correlation (HMBC) spectrum showed correlations between C H-1:C-1 and A H-2:C-2 and between B H-1:C-1 and A H-4:C-4. These data fit the structure β-D-Gal*p*-(1→2)[β-D-Gal*p*-(1→4)]Glc-ol. For structure 13_r, H-2:C-2 and H-6a/b:C-6 are significantly shifted, indicating substitution at these positions. The HMBC spectrum showed correlations between B H-1:C-1 and A H-6a/b:C-6 and between C H-1:C-1 and A H-2:C-2, confirming the disubstitution of glucitol residue A. These data lead to structure β-D-Gal*p*-(1→2)[β-D-Gal*p*-(1→6)]-Glc-ol. Structure 21_r showed only a shifted H-4;C-4 in the glucitol residue, fitting a monosubstituted glucitol residue. Residue B showed a chemical shift pattern matching a 4-substituted β-D-Gal*p* residue, while residue C matched with a terminal β-D-Gal*p* residue (Table S1 of the Supporting Information). These data lead to a β-D-Gal*p*-(1→4)-β-D-Gal*p*-(1→4)-Glc-ol structure. The NMR spectra of structure 13_n matched exactly with data for the non-reducing GOS structure β-D-Gal*p*-(1→4)-α-D-Glc*p*-(1↔1)-β-D-Gal*p* reported previously.[10]

3.2.2. Ratio of Galactose and Glucose Monomers in Vivinal GOS DP3. Theoretically both glucose and galactose could be present at the reducing end of GOS, because lactose, galactose, and glucose can serve as an acceptor for the enzyme−galactose complex in the transgalactosylation reaction.[29] In contrast to NMR, UHPLC−PGC−MS analysis does not allow for the conclusive differentiation between galactose and glucose monomers. Therefore, the monosaccharide composition of Vivinal GOS DP3 was determined using hydrolysis prior to HPAEC analysis. Galactose and glucose are present in a 2.1:1 ratio in Vivinal GOS DP3. This means that only 3.4% of all GOS DP3 isomers is composed of three galactose monomers. The preference for glucose or lactose as an acceptor in the transgalactosylation reaction was supported by previous in-depth characterization of Vivinal GOS, where the presence of isomers with galactose at the reducing end was limited to DP2.[8] For further characterization using UHPLC−PGC−MS, it is thus assumed that glucose is present at the reducing end of the GOS DP3 isomers.

3.2.3. Characterization of DP3 Isomers Using UHPLC−PGC−MS. Analytical UHPLC−PGC−MS was used for the characterization of reducing and non-reducing GOS DP3 isomers present in Vivinal GOS. First of all, β-3′-galactosyl-lactose (20_r in Figure 2), β-4′-galactosyl-lactose (10_r in Figure 2), and β-6′-galactosyl-lactose (18_r in Figure 2) were

https://dx.doi.org/10.1021/acs.jafc.0c02684
J. Agric. Food Chem. 2020, 68, 7800−7808

characterized on the basis of the comparison of the retention time and MS^2 fragmentation to those of the corresponding commercial standards.

Linkage-specific cross-ring MS^2 fragmentation was investigated to determine $\beta(1-4)$ and $\beta(1-6)$ linkages as described in previous studies of GOS.[30,31] The fragment ions are described according to the nomenclature of Domon and Costello.[32] The presence of $^{0,2}A_2(-H_2O)$ and the absence of $^{0,3}A_2$ cross-ring fragments indicate $\beta(1-4)$ linkages, whereas the presence of $^{0,3}A_2$ and the absence of $^{0,2}A_2(-H_2O)$ cross-ring fragments indicate $\beta(1-6)$ linkages, with ions at m/z 263 for $^{0,2}A_2(-H_2O)$ and m/z 251 for $^{0,3}A_2$ cross-ring fragments in negative ionization mode.[30,31] These MS fragmentation rules were confirmed by the MS fragmentation behavior of known GOS DP3 structures present in pure form. Unfortunately, these rules are only applicable for linkage identification at the non-reducing end as a result of the disappearance of the ring structure upon reduction. Nonetheless, these MS fragmentation rules resulted in the partial characterization of four reducing isomers, 3_r, 5_r, 7_r, and 14_r (Figure 2), representing β-D-Gal$p$-(1→6)-β-D-Gal$p$-(1→X)-D-Glc, β-D-Gal$p$-(1→6)-β-D-Gal$p$-(1→X)-D-Glc, β-D-Gal$p$-(1→4)-β-D-Gal$p$-(1→3/6)-D-Glc, and β-D-Gal$p$-(1→6)-β-D-Gal$p$-(1→X)-D-Glc, respectively. MS^2 fragmentation of GOS DP3 isomers is summarized in Table S2 of the Supporting Information.

Furthermore, a comparison of the MS^2 fragmentation spectra of the selected isomers characterized by NMR, 4_r, 21_r, 10_r, and 13_r, resulted in MS fragmentation rules to distinguish mono- and disubstitution of glucitol (Figure 5). The dominance of a Z_2 fragment with m/z 325 indicates disubsitituted glucitol, whereas the dominance of the Y_2 fragment with m/z 343 indicates monosubstituted glucitol with two consecutive galactose units. In total, 7 of 23 reducing GOS DP3 isomers are composed of disubstituted glucitol. The fragmentation rule can also be applied to higher DPs. For reducing GOS DP4 isomers, clear differences in relative abundance were observed between Z_3 (m/z 487) and Y_3 (m/z 505) fragments in the mass spectra (Table S3 of the Supporting Information). Interestingly, also for DP4, 7 isomers with a disubstitution were detected. Additionally, PGC elution patterns were comparable for DP3 and DP4, with on average lower retention times for disubstituted isomers. Taking into account the presence of a homologous series, these findings suggest that, also for DP4, disubstitution is located at the glucitol residue.

For the characterization of the non-reducing DP3 isomers, the same cross-ring MS fragmentation rules were applied. MS^2 fragmentation did not provide conclusive information on the type of linkage or monomers present in each non-reducing isomer. Nonetheless, in total, 6 non-reducing isomers with a $\beta(1-4)$ linkage and 2 non-reducing isomers with a $\beta(1-6)$ linkage were identified.

An overview of all conclusively and tentatively characterized or unknown GOS isomers is shown in Tables 1 and 2 for reducing and non-reducing isomers, respectively. Peak numbers correspond to numbered peaks in Figure 2. In total, 29 of 38 reducing and non-reducing GOS DP3 isomers were partially or completely characterized. The developed characterization method based on UHPLC−PGC−MS thus showed us that Vivinal GOS DP3 is highly diverse.

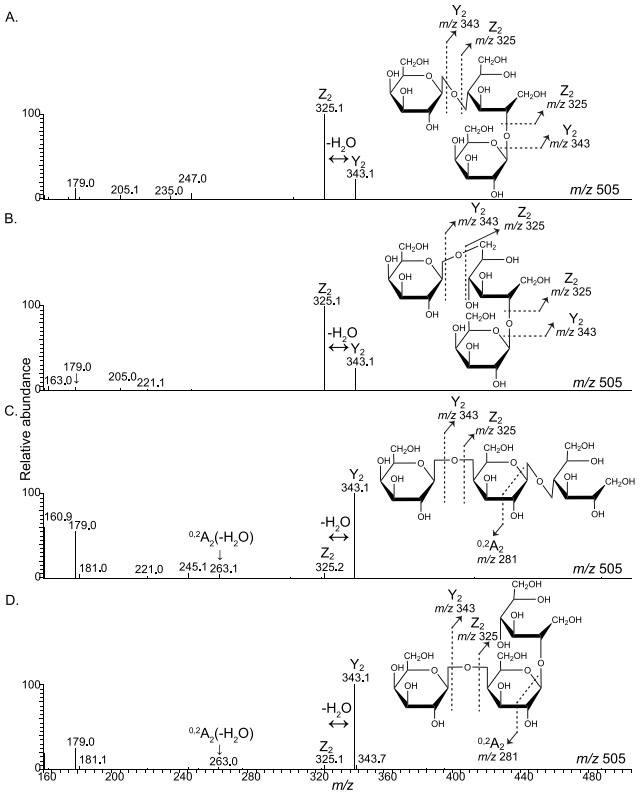

Figure 5. Fragmentation spectra (ESI MS^2) in negative mode of GOS DP3 isomers (A) 4_r, (B) 21_r, (C) 10_r, and (D) 13_r. The proposed routes of formation of the fragment ions, which are used to distinguish reducing isomers with mono- and disubstituted glucitol, are indicated in the spectra. The fragment ions are described according to the nomenclature of Domon and Costello.[32]

4. DISCUSSION

The glycosidic linkage and DP of GOS affect their bioactivity, as observed for fermentability and consequent health effects,[14−18] but solid evidence for these structure−function relationships is still limited. This is partially due to the high complexity of GOS with several GOS isomers present per DP. In this study, a high-throughput characterization method based on UHPLC−PGC−MS was developed to enable efficient screening of structure-specific health effects of Vivinal GOS. The method focuses on GOS DP3 isomers but will also provide insight into the structure of higher DPs because it was previously shown that higher DPs are mainly $\beta(1-4)$ elongations of DP3 isomers by β-D-Gal$p$.[8] Our study corroborates this finding because the number of isomers detected did not increase for DP4 and DP5.

UHPLC−PGC was shown to be highly valuable for the recognition of the different isomers present in Vivinal GOS. The complex retention mechanism of PGC based on both the size and planarity of neutral oligosaccharides[33] resulted in the excellent separation of 38 GOS DP3 isomers. A previous study using nano-PGC−LC only found 14 GOS DP3 isomers and did not notice further characterization.[22] Other chromatographic techniques, such as HPAEC−PAD and HILIC−MS, resulted in an inadequate separation because 11 and 5 GOS DP3 isomers were detected, respectively.[9,13] Also, for DP4 and DP5, UHPLC−PGC surpassed the chromatographic resolution of the aforementioned techniques. In total, 34 and 35 GOS DP4 and DP5 isomers were separated using UHPLC−

https://dx.doi.org/10.1021/acs.jafc.0c02684
J. Agric. Food Chem. 2020, 68, 7800−7808

Table 1. Overview of Conclusively and Tentatively Characterized or Unknown Reducing GOS DP3 Isomers

peak no.	graphical structure[a]	relative abundance (%)[b]	substitution glucitol	chemical structure[c]
1r		0.2	disubstituted	X
2r		0.1	disubstituted	X
3r		0.1	monosubstituted	(1→6)(1→X)
4r		2.3	disubstituted	β-D-Galp-(1→2)-[β-D-Galp-(1→4)-]D-Glc
5r		1.3	monosubstituted	(1→6)(1→X)
6r		0.2	disubstituted	X
7r	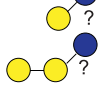	1.4	monosubstituted	(1→4)(1→3/6)
8r	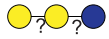	0.6	monosubstituted	X
9r		0.5	monosubstituted	X
10r	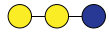	37.8	monosubstituted	β-D-Galp-(1→4)-β-D-Galp-(1→4)-D-Glc
11r		1.5	disubstituted	X
12r		2.8	monosubstituted	X
13r		11.2	monosubstituted	β-D-Galp-(1→4)-β-D-Galp-(1→2)-D-Glc
14r		1.6	monosubstituted	(1→6)(1→X)
15r		0.3		X
16r	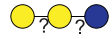	8.9	monosubstituted	X
17r		8.2	disubstituted	X
18r		2.9	monosubstituted	β-D-Galp-(1→6)-β-D-Galp-(1→4)-D-Glc
19r		0.6		X
20r	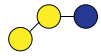	1.4	monosubstituted	β-D-Galp-(1→3)-β-D-Galp-(1→4)-D-Glc
21r		2.3	disubstituted	β-D-Galp-(1→2)-[β-D-Galp-(1→6)-]D-Glc
22r	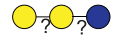	0.7	monosubstituted	X
23r		1.1	monosubstituted	X

[a]Included for conclusively and tentatively characterized isomers: yellow, galactose; blue, glucose; and ?, unknown type of glycosidic linkage. [b]Determined by integration of peak areas in UHPLC−PGC−MS with the sum of both reducing and non-reducing DP3 isomers set at 100%. [c]X = unknown.

PGC, whereas less than 14 and 10 DP4 and DP5 isomers were detected using HPAEC−PAD and HILIC−MS.[9,13]

NMR was used to characterize GOS DP3 isomers representing different isomer classes. The combination of SEC and preparative PGC−MS resulted in 4 pure isomers, which were successfully characterized by NMR: the reducing isomers *β*-D-Gal*p*-(1→2)-[*β*-D-Gal*p*-(1→4)-]D-Glc, *β*-D-Gal*p*-(1→4)-*β*-D-Gal*p*-(1→2)-D-Glc, and *β*-D-Gal*p*-(1→2)-[*β*-D-Gal*p*-(1→6)-]D-Glc and the non-reducing isomer *β*-D-Gal*p*-(1→4)-*α*-D-Glc*p*-(1↔1)-*β*-D-Gal*p*. The characterized isomers confirmed structures reported in previous studies.[8,10] Consequently, they will serve as "standards" to further develop the high-throughput characterization method based on UHPLC−PGC−MS. The laborious fractionation steps prior to analysis would be unnecessary once having such a LC−MS method.

Reflection of the fragmentation behavior of the characterized isomers led to the discovery of a MS fragmentation rule to distinguish reducing isomers with mono- and disubstituted glucitol. The type of linkage was determined using the linkage-specific cross-ring MS^2 fragments at the non-reducing end.[30,31] These two MS fragmentation rules resulted in the partial characterization of 23 of 38 GOS DP3 isomers. Interestingly,

https://dx.doi.org/10.1021/acs.jafc.0c02684
J. Agric. Food Chem. 2020, 68, 7800−7808

Table 2. Overview of Conclusively and Tentatively Characterized or Unknown Non-reducing GOS DP3 Isomers

peak no.	graphical structure[a]	relative abundance (%)[b]	chemical structure[c]
1_n		0.1	X
2_n		0.04	(1→4)(1↔1) / (1↔1)(4←1)
3_n		0.6	X
4_n		0.6	(1→4)(1↔1) / (1↔1)(4←1)
5_n		0.1	(1→6)(1↔1) / (1↔1)(6←1)
6_n		0.2	(1→4)(1↔1) / (1↔1)(4←1)
7_n		0.2	X
8_n		1.5	(1→4)(1↔1) / (1↔1)(4←1)
9_n		0.2	X
10_n		3.7	(1→4)(1↔1) / (1↔1)(4←1)
11_n		0.2	X
12_n		0.5	(1→6)(1↔1) / (1↔1)(6←1)
13_n	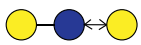	3.9	β-D-Galp-(1→4)-α-D-Glcp-(1↔1)-β-D-Galp
14_n		0.3	X
15_n		0.2	X

[a]Included for conclusively characterized isomers: yellow, galactose; blue, glucose. [b]Determined by integration of peak areas in UHPLC−PGC−MS with the sum of both reducing and non-reducing DP3 isomers set at 100%. [c]X = unknown.

MS^2 fragmentation spectra of GOS DP4 illustrated that the fragmentation rules are also applicable to higher DPs for the determination of the substitution of glucitol as well as for the type of glycosidic linkages.

The clear-cut distinction between reducing and non-reducing isomers on the m/z value made it a straightforward approach to recognize the 15 GOS DP3 isomers with a (1−1) linkage. A couple of non-reducing isomers have been reported in previous studies regarding the characterization of Vivinal GOS.[8−10] However, these studies required labor-intensive fractionation techniques prior to characterization of the non-reducing isomers by NMR analysis. In this study, MS^2 fragmentation analysis revealed 6 non-reducing DP3 isomers with a (1−4) linkage. β(1−4)-linked galactose can be connected to (1−1)-linked glucose as observed for isomer 13_n: β-D-Gal*p*-(1→4)-α-D-Glc*p*-(1↔1)-β-D-Gal*p*. Next, it is hypothesized that β(1−4)-linked galactose can also be connected to (1−1)-linked galactose, resulting in α-D-Glc*p*-(1↔1)-β-D-Gal*p*-(4←1)-β-D-Gal*p*. The study of Fransen et al.[10] corroborates this hypothesis because they reported on the presence of non-reducing DP4 and DP5 GOS isomers consisting of β(1−4)-linked galactose connected to a (1−1)-linked galactose unit: β-D-Gal*p*-(1→4)-α-D-Glc*p*-(1↔1)-β-D-Gal*p*-(4←1)-β-D-Gal*p* and β-D-Gal*p*-(1→4)-α-D-Glc*p*-(1↔1)-β-D-Gal*p*-(4←1)-β-D-Gal*p*-(4←1)-β-D-Gal*p*. The large variety of non-reducing DP3 isomers can be further explained by the presence of a structural motif containing solely β linkages, such as β-D-Glc*p*-(1↔1)-β-D-Gal*p*, as shown in previous research for GOS DP2.[9]

The complete characterization of Vivinal GOS DP3 by solely UHPLC−PGC−MS is still impeded by the challenge to distinguish galactose/glucose and α/β linkages based on MS^2 fragmentation. Furthermore, an optimal separation of the numerous GOS structures on PGC demands reduction of the reducing end prior to analysis, which results in the lack of linkage-specific cross-ring fragments of resulting terminal glucitol. More studies should be performed on alternative labeling techniques of GOS to obtain both optimal chromatographic separation and informative MS^2 fragmentation spectra.

Nevertheless, the established high-throughput characterization method based on UHPLC−PGC−MS will already have important implications for future structure−function studies on GOS because it provides deeper insight in the complexity of the GOS mixtures. In particular, the fragmentation rule to distinguish mono- and disubstituted glucitol turned out to be highly relevant because ongoing research revealed a difference in resistance to fermentation by infant fecal microbiota (results not shown).

The characterization method also shed light on the high diversity of non-reducing GOS isomers. The identification of non-reducing GOS isomers is hindered in currently used methods as a result of their co-elution with more abundant isomers. Hence, little is known about the fermentability and health effects of these specific structures. To our knowledge, only one study reported on the hydrolysis of non-reducing GOS DP2 by bacterial enzymes.[34] Nonetheless, with 12%, the non-reducing isomers make up a considerable part of GOS DP3 and can therefore not be ignored. UHPLC−PGC−MS

https://dx.doi.org/10.1021/acs.jafc.0c02684
J. Agric. Food Chem. 2020, 68, 7800−7808

readily facilitates incorporation in future structure−function studies.

In summary, analytical UHPLC−PGC−MS has proven to be a powerful tool to touch upon the high complexity of Vivinal GOS. More than 100 different Vivinal GOS structures were separated in one single run by the separation mechanism of UHPLC−PGC−MS. In total, 23 reducing and 15 non-reducing DP3 isomers were identified, which shows us that Vivinal GOS is structurally much more diverse than previously noticed. The established characterization method facilitates the detection of non-reducing GOS and several structural features of GOS, which could impact the fermentability by infant gut microbiota. Hence, this study will contribute to a deeper understanding of the structure-specific utilization of GOS by infant gut microbiota and consequent health effects.

■ ASSOCIATED CONTENT

Supporting Information

The Supporting Information is available free of charge at https://pubs.acs.org/doi/10.1021/acs.jafc.0c02684.

Chemical shifts for GOS DP3 isomer 4_r, 13_r, 21_r, and 13_n determined from one-dimensional (1D) and two-dimensional (2D) NMR spectra (Table S1), overview of characterized reducing and non-reducing DP3 GOS isomers (Table S2), and fragmentation behavior of reducing GOS DP4 isomers (Table S3) (PDF)

■ AUTHOR INFORMATION

Corresponding Author

Henk A. Schols − *Laboratory of Food Chemistry, Wageningen University & Research, 6708 WG Wageningen, Netherlands;* orcid.org/0000-0002-5712-1554; Phone: +31-317-482239; Email: henk.schols@wur.nl

Authors

Madelon J. Logtenberg − *Laboratory of Food Chemistry, Wageningen University & Research, 6708 WG Wageningen, Netherlands*

Kristel M. H. Donners − *Laboratory of Food Chemistry, Wageningen University & Research, 6708 WG Wageningen, Netherlands*

Jolien C. M. Vink − *Laboratory of Food Chemistry, Wageningen University & Research, 6708 WG Wageningen, Netherlands*

Sander S. van Leeuwen − *Cluster Human Nutrition & Health, Department of Laboratory Medicine, University Medical Center Groningen, 9713 GZ Groningen, Netherlands;* orcid.org/0000-0003-0017-2841

Pieter de Waard − *Magnetic Resonance Research Facility (MAGNEFY), Wageningen University & Research, 6708 WE Wageningen, Netherlands*

Paul de Vos − *Immunoendocrinology, Department of Pathology and Medical Biology, University of Groningen and University Medical Centre Groningen, 9700 RB Groningen, Netherlands*

Complete contact information is available at: https://pubs.acs.org/10.1021/acs.jafc.0c02684

Funding

Research by Madelon J. Logtenberg was performed in the public−private partnership "CarboKinetics" coordinated by the Carbohydrate Competence Center (CCC, www.cccresearch.nl). CarboKinetics is financed by participating industrial partners Agrifirm Innovation Center B.V., Cooperatie Avebe U.A., DSM Food Specialties B.V., FrieslandCampina Nederland B.V., Nutrition Sciences N.V., VanDrie Holding N.V., and Sensus B.V. and allowances of The Netherlands Organisation for Scientific Research (NWO).

Notes

The authors declare no competing financial interest.

■ ACKNOWLEDGMENTS

The authors thank Edwin Bakx (Laboratory of Food Chemistry, Wageningen University) for the fruitful discussions on the interpretation of the mass spectra.

■ ABBREVIATIONS USED

ACN, acetonitrile; D_2O, deuterium oxide; DP, degree of polymerization; FL, fucosyllactose; FOS, fructo-oligosaccharides (synonym oligofructose); GOS, galacto-oligosaccharides; HILIC, hydrophilic interaction chromatography; HMBC, heteronuclear multiple-bond correlation; HMO, human milk oligosaccharides; HPAEC−PAD, high-performance anion-exchange chromatography with pulsed amperometric detection; LNT, lacto-*N*-tetraose; MALDI−TOF−MS, matrix-assisted laser desorption/ionization time-of-flight mass spectrometry; $NaBH_4$, sodium borohydrate; RI, refractive index; SEC, size-exclusion chromatography; SL, sialyllactose; SPE, solid-phase extraction; TFA, trifluoroacetic acid; UHPLC−PGC−MS, ultra-high-performance liquid chromatography with porous graphitic carbon coupled to mass spectrometry

■ REFERENCES

(1) Matamoros, S.; Gras-Leguen, C.; Le Vacon, F.; Potel, G.; de La Cochetiere, M.-F. Development of intestinal microbiota in infants and its impact on health. *Trends Microbiol.* **2013**, *21* (4), 167−173.

(2) Marques, T. M.; Wall, R.; Ross, R. P.; Fitzgerald, G. F.; Ryan, C. A.; Stanton, C. Programming infant gut microbiota: Influence of dietary and environmental factors. *Curr. Opin. Biotechnol.* **2010**, *21* (2), 149−156.

(3) Smilowitz, J. T.; Lebrilla, C. B.; Mills, D. A.; German, J. B.; Freeman, S. L. Breast milk oligosaccharides: Structure−function relationships in the neonate. *Annu. Rev. Nutr.* **2014**, *34*, 143−69.

(4) Holscher, H. D.; Bode, L.; Tappenden, K. A. Human milk oligosaccharides influence intestinal epithelial cell maturation *in vitro*. *J. Pediatr. Gastroenterol. Nutr.* **2017**, *64* (2), 296−301.

(5) Bych, K.; Mikš, M. H.; Johanson, T.; Hederos, M. J.; Vigsnæs, L. K.; Becker, P. Production of HMOs using microbial hosts—From cell engineering to large scale production. *Curr. Opin. Biotechnol.* **2019**, *56*, 130−137.

(6) Verkhnyatskaya, S.; Ferrari, M.; de Vos, P.; Walvoort, M. T. C. Shaping the infant microbiome with non-digestible carbohydrates. *Front. Microbiol.* **2019**, *10*, 343.

(7) Torres, D. P. M.; Gonçalves, M. d. P. F.; Teixeira, J. A.; Rodrigues, L. R. Galacto-oligosaccharides: Production, properties, applications, and significance as prebiotics. *Compr. Rev. Food Sci. Food Saf.* **2010**, *9* (5), 438−454.

(8) van Leeuwen, S. S.; Kuipers, B. J.; Dijkhuizen, L.; Kamerling, J. P. 1 H NMR analysis of the lactose/*β*-galactosidase-derived galacto-oligosaccharide components of Vivinal® GOS up to DP5. *Carbohydr. Res.* **2014**, *400*, 59−73.

(9) Coulier, L.; Timmermans, J.; Bas, R.; Van Den Dool, R.; Haaksman, I.; Klarenbeek, B.; Slaghek, T.; Van Dongen, W. In-depth characterization of prebiotic galacto-oligosaccharides by a combination of analytical techniques. *J. Agric. Food Chem.* **2009**, *57* (18), 8488−95.

(10) Fransen, C. T.; Van Laere, K. M.; van Wijk, A. A.; Brull, L. P.; Dignum, M.; Thomas-Oates, J. E.; Haverkamp, J.; Schols, H. A.; Voragen, A. G.; Kamerling, J. P.; Vliegenthart, J. F. alpha-D-Glcp-(1−1)-beta-D-Galp-containing oligosaccharides, novel products from

lactose by the action of beta-galactosidase. *Carbohydr. Res.* **1998**, *314* (1−2), 101−14.
(11) Yin, H.; Bultema, J. B.; Dijkhuizen, L.; van Leeuwen, S. S. Reaction kinetics and galactooligosaccharide product profiles of the β-galactosidases from *Bacillus circulans Kluyveromyces lactis* and *Aspergillus oryzae*. *Food Chem.* **2017**, *225*, 230−238.
(12) van Leeuwen, S. S.; Kuipers, B. J. H.; Dijkhuizen, L.; Kamerling, J. P. Comparative structural characterization of 7 commercial galacto-oligosaccharide (GOS) products. *Carbohydr. Res.* **2016**, *425*, 48−58.
(13) Hernández-Hernández, O.; Calvillo, I.; Lebrón-Aguilar, R.; Moreno, F. J.; Sanz, M. L. Hydrophilic interaction liquid chromatography coupled to mass spectrometry for the characterization of prebiotic galactooligosaccharides. *J. Chromatogr. A* **2012**, *1220*, 57−67.
(14) Ladirat, S.; Schols, H.; Nauta, A.; Schoterman, M.; Schuren, F.; Gruppen, H. *In vitro* fermentation of galacto-oligosaccharides and its specific size-fractions using non-treated and amoxicillin-treated human inoculum. *Bioact. Carbohydr. Diet. Fibre* **2014**, *3* (2), 59−70.
(15) Difilippo, E.; Pan, F.; Logtenberg, M.; Willems, R.; Braber, S.; Fink-Gremmels, J.; Schols, H. A.; Gruppen, H. *In vitro* fermentation of porcine milk oligosaccharides and galacto-oligosaccharides using piglet fecal inoculum. *J. Agric. Food Chem.* **2016**, *64* (10), 2127−2133.
(16) Akbari, P.; Fink-Gremmels, J.; Willems, R. H. A. M.; Difilippo, E.; Schols, H. A.; Schoterman, M. H. C.; Garssen, J.; Braber, S. Characterizing microbiota-independent effects of oligosaccharides on intestinal epithelial cells: Insight into the role of structure and size: Structure−activity relationships of non-digestible oligosaccharides. *Eur. J. Nutr.* **2017**, *56* (5), 1919−1930.
(17) Depeint, F.; Tzortzis, G.; Vulevic, J.; I'Anson, K.; Gibson, G. R. Prebiotic evaluation of a novel galactooligosaccharide mixture produced by the enzymatic activity of *Bifidobacterium bifidum* NCIMB 41171, in healthy humans: A randomized, double-blind, crossover, placebo-controlled intervention study. *Am. J. Clin. Nutr.* **2008**, *87* (3), 785−91.
(18) Rodriguez-Colinas, B.; Kolida, S.; Baran, M.; Ballesteros, A. O.; Rastall, R. A.; Plou, F. J. Analysis of fermentation selectivity of purified galacto-oligosaccharides by *in vitro* human faecal fermentation. *Appl. Microbiol. Biotechnol.* **2013**, *97* (13), 5743−52.
(19) Yin, H.; Pijning, T.; Meng, X.; Dijkhuizen, L.; van Leeuwen, S. S. Engineering of the *Bacillus circulans* beta-galactosidase product specificity. *Biochemistry* **2017**, *56* (5), 704−711.
(20) Ruhaak, L. R.; Deelder, A. M.; Wuhrer, M. Oligosaccharide analysis by graphitized carbon liquid chromatography−mass spectrometry. *Anal. Bioanal. Chem.* **2009**, *394* (1), 163−174.
(21) Bao, Y.; Chen, C.; Newburg, D. S. Quantification of neutral human milk oligosaccharides by graphitic carbon high-performance liquid chromatography with tandem mass spectrometry. *Anal. Biochem.* **2013**, *433* (1), 28−35.
(22) Peacock, K. S.; Ruhaak, L. R.; Tsui, M. K.; Mills, D. A.; Lebrilla, C. B. Isomer-specific consumption of galactooligosaccharides by bifidobacterial species. *J. Agric. Food Chem.* **2013**, *61* (51), 12612−12619.
(23) Ni, W.; Bones, J.; Karger, B. L. In-depth characterization of N-linked oligosaccharides using fluoride-mediated negative ion microfluidic chip LC-MS. *Anal. Chem.* **2013**, *85* (6), 3127−35.
(24) Konda, C.; Londry, F. A.; Bendiak, B.; Xia, Y. Assignment of the stereochemistry and anomeric configuration of sugars within oligosaccharides via overlapping disaccharide ladders using MSn. *J. Am. Soc. Mass Spectrom.* **2014**, *25* (8), 1441−1450.
(25) Duus, J.; Gotfredsen, C. H.; Bock, K. Carbohydrate structural determination by NMR spectroscopy: Modern methods and limitations. *Chem. Rev.* **2000**, *100* (12), 4589−614.
(26) Jonathan, M. C.; van Brussel, M.; Scheffers, M. S.; Kabel, M. A. Characterisation of branched gluco-oligosaccharides to study the mode-of-action of a glucoamylase from *Hypocrea jecorina*. *Carbohydr. Polym.* **2015**, *132*, 59−66.
(27) Logtenberg, M. J.; Vink, J. C. M.; Serierse, R. M.; An, R.; Hermes, G. D. A.; Smidt, H.; Schols, H. A. Pooled faecal inoculum can predict infant prebiotic fermentability despite high inter-individual variability of microbiota composition. **2020**, manuscript submitted.
(28) Wishart, D. S.; Feunang, Y. D.; Marcu, A.; Guo, A. C.; Liang, K.; Vazquez-Fresno, R.; Sajed, T.; Johnson, D.; Li, C.; Karu, N.; Sayeeda, Z.; Lo, E.; Assempour, N.; Berjanskii, M.; Singhal, S.; Arndt, D.; Liang, Y.; Badran, H.; Grant, J.; Serra-Cayuela, A.; Liu, Y.; Mandal, R.; Neveu, V.; Pon, A.; Knox, C.; Wilson, M.; Manach, C.; Scalbert, A. HMDB 4.0: The human metabolome database for 2018. *Nucleic Acids Res.* **2018**, *46* (D1), D608−d617.
(29) Warmerdam, A.; Zisopoulos, F. K.; Boom, R. M.; Janssen, A. E. Kinetic characterization of galacto-oligosaccharide (GOS) synthesis by three commercially important beta-galactosidases. *Biotechnol. Prog.* **2014**, *30* (1), 38−47.
(30) Guan, B.; Cole, R. B. MALDI linear-field reflectron TOF post-source decay analysis of underivatized oligosaccharides: Determination of glycosidic linkages and anomeric configurations using anion attachment. *J. Am. Soc. Mass Spectrom.* **2008**, *19* (8), 1119−1131.
(31) Black, B. A.; Lee, V. S.; Zhao, Y. Y.; Hu, Y.; Curtis, J. M.; Gänzle, M. G. Structural identification of novel oligosaccharides produced by *Lactobacillus bulgaricus* and *Lactobacillus plantarum*. *J. Agric. Food Chem.* **2012**, *60* (19), 4886−4894.
(32) Domon, B.; Costello, C. E. A systematic nomenclature for carbohydrate fragmentations in FAB-MS/MS spectra of glycoconjugates. *Glycoconjugate J.* **1988**, *5* (4), 397−409.
(33) Bapiro, T. E.; Richards, F. M.; Jodrell, D. I. Understanding the complexity of Porous Graphitic Carbon (PGC) chromatography: Modulation of mobile-stationary phase interactions overcomes loss of retention and reduces variability. *Anal. Chem.* **2016**, *88* (12), 6190−4.
(34) Van Laere, K. M.; Abee, T.; Schols, H. A.; Beldman, G.; Voragen, A. G. Characterization of a novel beta-galactosidase from *Bifidobacterium adolescentis* DSM 20083 active towards trans-galactooligosaccharides. *Appl. Environ. Microbiol.* **2000**, *66* (4), 1379−1384.

https://dx.doi.org/10.1021/acs.jafc.0c02684
J. Agric. Food Chem. 2020, 68, 7800−7808